HHS Public Access

Author manuscript

J Am Chem Soc. Author manuscript; available in PMC 2022 December 16.

Harzianic Acid from *Trichoderma afroharzianum* is a Natural Product Inhibitor of Acetohydroxyacid Synthase

Linan Xie[†,$,#], **Xin Zang**[§,#], **Wei Cheng**[†,&], **Zhuan Zhang**[‖], **Jiahai Zhou**[*,§,⊥], **Mengbin Chen**[*,†], **Yi Tang**[*,†,‡]

[†]Department of Chemical and Biomolecular Engineering, University of California Los Angeles, Los Angeles, California 90095, United States,

[‡]Chemistry and Biochemistry, University of California Los Angeles, Los Angeles, California 90095, United States,

[$]Biotechnology Research Institute, The Chinese Academy of Agricultural Sciences, 12 Zhongguancun South Street, Beijing 100081, P.R. China,

[§]State Key Laboratory of Bio-organic and Natural Products Chemistry, Center for Excellence in Molecular Synthesis, Shanghai Institute of Organic Chemistry, University of Chinese Academy of Sciences, Shanghai 200032, China,

[&]State Key Laboratory of Natural and Biomimetic Drugs, Peking University, Beijing 100191, China,

[⊥]CAS Key Laboratory of Quantitative Engineering Biology, Shenzhen Institute of Synthetic Biology, Shenzhen Institute of Advanced Technology, Chinese Academy of Sciences, Shenzhen 518055, China,

[‖]Texas Therapeutics Institute, the Brown Foundation Institute of Molecular Medicine, The University of Texas Health Science Center at Houston, Houston, Texas 77054, United States.

Abstract

Acetohydroxyacid synthase (AHAS) is the first enzyme in the branched-chain amino acid biosynthetic pathway, and is a validated target for herbicide and fungicide development. Here we report harzianic acid (HA, **1**) produced by the biocontrol fungus *Trichoderma afroharzianum* t-22 (Tht22) as a natural product inhibitor of AHAS. The biosynthetic pathway of HA was elucidated with heterologous reconstitution. Guided by a putative self-resistance enzyme in the genome, HA was biochemically demonstrated to be a selective inhibitor of fungal AHAS, including those from phytopathogenic fungi. In addition, HA can inhibit the common resistant variant of AHAS in which the active site proline is mutated. Structural analysis of AHAS complexed with HA revealed the molecular basis of the competitive inhibition, which differs from all known commercial AHAS inhibitors. The alternative binding mode also rationalizes selectivity of HA, as well as

[*]Corresponding authors: Yi Tang, yitang@ucla.edu, 420 Westwood Plaza, Los Angeles, CA 90095, USA; Mengbin Chen, mengbinchen@ucla.edu, 420 Westwood Plaza, Los Angeles, CA 90095, USA; Jiahai Zhou, jiahai@mail.siat.ac.cn, 1068 Xueyuan Avenue, Shenzhen University Town, Shenzhen, P. R. China.
[#]These authors contributed equally.

Supporting Information

Experimental details, spectroscopic data. This material is available free of charge via the Internet at http://pubs.acs.org.

The authors declare no competing financial interest.

effectiveness towards resistant mutants. A proposed role of HA biosynthesis by Tht22 in the rhizosphere is discussed based on the data.

Graphical Abstract

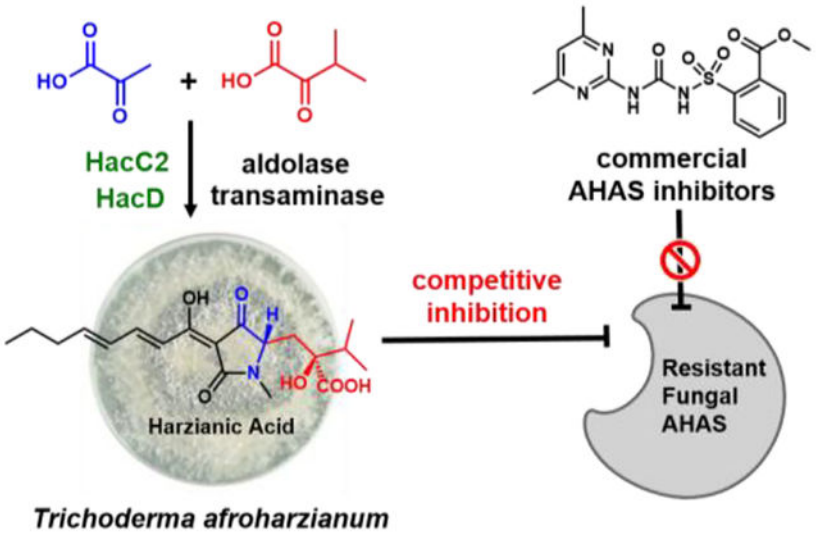

INTRODUCTION

Secondary metabolites biosynthesized by microbes, also known as natural products, are small molecules that have a wide range of biological activities.[1–2] The importance of secondary metabolites in treating human diseases is well-documented, and has been a driving force for their continual discovery. These molecules also play indispensable roles in agriculture, as many frontline pesticides are natural products or derivatives thereof.[3–5] In the plant rhizosphere where microbial communities interact with each other and with plant roots, secreted secondary metabolites can significantly impact plant health both beneficially and deleteriously.[6] For example, root-colonizing fungi can directly synthesize plant phytohormones, such as abscisic acid[7] and gibberellins[8–9] to affect the balance between plant growth and stress responses. In addition, plant-benefiting microbes can biosynthesize antimicrobials to limit the growth of plant pathogens, contributing to the overall fitness of the plant.[10–11] A complete understanding of rhizosphere secondary metabolites, including their biosynthesis and biological activities, will therefore contribute to the discovery of new agrochemicals.

Towards this end, we have focused on secondary metabolites from *Trichoderma harzianum* t-22 (Tht22, which has been reclassified as *Trichoderma afroharzianum*) used in fungal plant pathogen biocontrol.[12] The root-colonizing Tht22 has major influences on soil microbe composition, nutrient uptake, and innate plant signaling pathways related to immunity and development.[13–15] Tht22 has been shown to decrease the incidence and severity of agriculturally relevant diseases, such as wilt, mildew, and rice blast.[10, 16–18] A number of natural products have been identified from Tht22, including abscisic acid,[19] antimicrobial trichosetin[20], growth promoting harzianolide,[21] and others.[22–23] The number

of known metabolites (<10) from Tht22, however, represents only a minor fraction of the biosynthetic gene clusters (BGCs) identified from the sequenced Tht22 genome (JGI Project ID: 1185335).[24] Using genome mining approaches, we previously discovered a Fe^{3+}-reducing metabolite tricholignan from Tht22,[25] demonstrating the potential of finding new modulators of plant-microbe or microbe-microbe interactions.

In this work, we aimed to understand the biosynthesis and potential biological activities of harzianic acid (HA, **1**), a natural product synthesized by Tht22 (Figure 1).[26] HA, originally isolated in 1994 from *Trichoderma harzianum* SY-307,[27] and re-isolated along with homoharzianic acid (**4**) and demethyharzianic acid (**5**) from other fungal strains,[28] is a *N*-methylated tetramic acid substituted with a dienoyl chain at C3' and an α-hydroxycarboxylate-containing aliphatic chain at C5'. HA displays a number of physical and biological properties that are relevant to Tht22-plant interactions. HA has an apparent binding constant (K_d) to Fe^{3+} of 1.79×10^{-25} M, and has been suggested to aid iron assimilation for plants.[29] HA displays antifungal activity against a number of plant pathogens, including *Pasteurekka piscicida sp*. 6395 (gram-negative bacterium), *Sclerotinia sclerotiorum*, and *Rhizoctonia solani* (plant pathogenic fungi).[26] When purified HA was applied to soybeans grown under greenhouse conditions, stem lengths were significantly improved (>40%). Under field conditions, production of soybean pods and seeds were increased by approximately 5–10% after applying HA.[30] At higher (10–100 μg) doses, growth inhibition of canola seedlings on petri dishes was observed.[26] While such findings indicate HA plays important roles in Tht22-plant interactions, the molecular target of HA remains elusive. In this work, we reconstituted the biosynthetic pathway of HA, and based on the presence of a potential self-resistance gene, we demonstrated HA as a new natural product inhibitor of acetohydroxyacid synthase (AHAS, also known as acetolactate synthase, ALS), the first enzyme in branched-chain amino acid biosynthesis. We showed that HA preferentially inhibits fungal AHASs, including those that have acquired resistant mutations to synthetic AHAS inhibitors widely used in the field.

RESULTS AND DISCUSSION

The Harzianic acid Biosynthesis Gene Cluster in Tht22.

HA is hypothesized to be biosynthesized from a hybrid polyketide synthase-nonribosomal peptide synthetase (PKS-NRPS) enzyme based on pathways of structurally related natural products such as equisetin (Figure 1).[31] The C5' carboxylate-containing substituent is derived from the unnatural amino acid 4-hydroxy-4-isopropyl glutamate (L-HIG), which is selected and activated by the adenylation domain of the NRPS module of the PKS-NRPS. The formation of L-HIG is likely to involve an aldolase−transaminase route, which was reported for the structurally related 4-hydroxyl-4-methyl glutamate (L-HMG) in biosynthesis of Sch210971.[32] In this two-step reaction, pyruvate and α-keto-isovalerate would undergo aldol condensation to form *S*-4-hydroxy-4-isopropyl-2-oxoglutarate (L-HIOG), followed by stereoselective transamination to give L-HIG. The PKS-NRPS would use malonyl-CoA and L-HIG as building blocks to generate a tetramic acid intermediate, which can be *N*-methylated by a methyltransferase to give HA. Guided by these proposed enzymatic

transformations, we searched the genome of Tht22 for a BGC encoding a PKR-NRPS, aldolase and transaminase.

Bioinformatic analysis of the Tht22 genome revealed that among the five Tht22 BGCs that encode an anchoring PKS-NRPS enzyme, only one has assigned function from a recent genome mining effort (Table S3).[33] The BGC located in contig 2 is the most suitable candidate for HA biosynthesis based on the above retrobiosynthetic analysis (Figure 2A), and is named the *hac* cluster. This cluster encodes a PKS-NRPS (*hacA*), a *trans*-acting enoylreductase (*hacB*) that partners with HacA, two predicted aldolases (*hacC1* and *hacC2*), an aminotransferase (*hacD*), and a *N*-methyltransferase (*hacE*). Among the two aldolases predicted from the cluster, HacC2 shows a higher sequence identity (61.6%) to the aldolase involved in L-HMG formation in the Sch210971 BGC.[32] The BGC also has a small gene *hacH* that encodes a protein with sequence homology to portions of the β-domain (FAD-binding site) of a canonical AHAS (Figure S1B)[34,35]. Two nearby genes, *hacF* and *hacG*, encode a transcriptional factor and transporter, respectively. Searching all sequenced fungal genomes revealed *Aspergillus ibericus* and *Penicillium digitatum*, as well as number of *Trichoderma* species encode homologous BGCs (Figure 2A and Table S4). Several key differences, however, are noted between the clusters. First, the BGC from *A. ibericus* encodes only one aldolase with strong sequence identity to HacC2; second, both homologous BGCs encode a full-length AHAS homolog ($AHAS^M$) compared to the truncated HacH ($AHAS^T$) in the Tht22 BGC.

Heterologous Biosynthesis of Harzianic Acid.

To investigate the biosynthesis pathway of the HA, we heterologously expressed the *hac* genes in the heterologous host *Aspergillus nidulans* A1145 ΔEMΔST.[36] Expressing the PKS-NRPS (HacA) and ER (HacB) did not produce any new metabolites compared to the empty vector controls (Figure 2B, trace i and ii). This can be attributed to the lack of the unnatural amino acid L-HIG to support steps catalyzed by the NRPS module of HacA. Based on the biosynthetic proposal, the combination of aldolase and transaminase should be sufficient to provide L-HIG. The two aldolases, HaC1 and HacC2, were individually coexpressed with HacA, HacB, and the transaminase (HacD). Coexpressing HacC2 led to formation of compounds **5–8** with λ_{max}=357 nm, with **5** being the dominant product (Figure 2B, trace iv). Compounds **5**–**8** were purified and the structures were elucidated by NMR analysis. **5** was confirmed to be demethylharzianic acid, which was previously isolated from fungus strain F-1531.[28] The minor compounds **6–8** are structurally related to **5** with the same tetramic acid core. NMR analysis (Table S10–S13, and Figures S23–S42) showed they differ in the length of the C7' alkyl unit (Figure 2C), which is consistent with the observed differences in retention times. Whereas **5** incorporates L-HIG, **6, 7**, and **8** incorporate 4-hydroxy-4-ethyl-glutamate (L-HEG), L-HMG, and 4-hydroxy-4-isobutyl-glutamate (L-HIBG), respectively. In contrast, no product was formed when HacC1 was coexpressed with HacA, HacB and HacD (Figure 2B, trace iii), suggesting HacC1 and HacC2 are not functionally redundant.

To obtain *N*-methylated **1**, we next coexpressed the *N*-methyltransferase (HacE) with HacA, HacB, HacC2 and HacD in *A. nidulans*. The strain produced **1** (λ_{max}=363 nm) at a titer

of 4.5 mg/L (Figure 2B, trace v, Tables S8–S9, and Figures S16–S22), together with a number of minor metabolites **2–4** (λ_{max}=363 nm) and **9–11** (λ_{max}=393 nm). NMR analysis confirmed the structure of **1** to be HA (Table S8–S9, and Figures S16–S22). Although **2–4** were not purified, the molecular weight and retention time differences indicate these are the *N*-methylated versions of **6–8**. Optical rotation measurements of **1** confirmed the stereochemistry of these compounds are consistent with the 5'*S* and 7'*S* reported for **1** isolated from Tht22, as well as from total synthesis.[26,37] To confirm the function and timing of HacE, we recombinantly expressed HacE from *Escherichia coli*, and performed enzymatic assay using **5–8** as substrates and *S*-adenosylmethionine (SAM) as cofactor. HacE was able to convert each compound to the *N*-methylated version with similar conversions (Figure S2). Due to the low titers of **9–11**, these compounds were not characterized by NMR. However, based on the +30 nm red-shifted λ_{max} and the molecular weights, we propose these to contain an additional conjugated olefin in the polyene portion of the molecules, possibly as a result of the ER (HacB) skipping the first programmed enoylreduction during PKS-NRPS function (Figure 2C).

Although HacC1 did not substitute the function of HacC2 in the above study, we examined its role in the biosynthesis of **1** by coexpressing the gene together with those produced **1–4** and **9–11**. Surprisingly, the coexpression of HacC1 significantly reduced the formation of the congeners of **1** in *A. nidulans* (Figure 2B, trace vi). This resulted in a heterologous host that produced **1** as the predominant product. Therefore, we propose that while HacC1 is not essential in the biosynthesis of **1**, the function of the enzyme can improve the substrate specificities of HacC2 and HacA. RT-PCR analysis of Tht22 under conditions when **1** is produced showed *hacC1* is not expressed (Figure S3), further suggesting the nonessential role of the enzyme. Its effect on product distribution could therefore be host-specific, and may reflect the differences in the pool of α-ketoacids in the heterologous host compared to that in Tht22. Lastly, we coexpressed the truncated $AHAS^T$ enzyme HacH with the other biosynthetic enzymes. As expected from sequence analysis which showed the active site residues are missing in this truncated enzyme, no effect on product formation can be observed (Figure 2B, trace vii).

The biosynthetic pathway of HA **1** is summarized in Figure 2C, which starts with the action of HacC2 in formation of L-HIOG from pyruvate and α-keto-isovalerate. After transamination catalyzed by HacD, the amino acid L-HIG is activated and selected by the NRPS module of HacA to condense with the dienone polyketide synthesized by the HRPKS module. Dieckmann cyclization of amidated polyketide yields the tetramic acid **5**, which is methylated by HacE to afford **1**.

AHAS as the Potential Target of Harzianic Acid.

Having established the link between the *hac* BGC and biosynthesis of **1**, we sought clues from the BGCs shown in Figure 1 for possible mode of action of **1**. The BGCs are well conserved with respect to the biosynthetic enzymes, with a notable exception that both *A. ibericus* and *P. digitatum* clusters contain a full length AHAS (named $AiAHAS^M$ and $PdAHAS^M$, respectively) compared to the truncated HacH in Tht22 ($AHAS^T$). Searching through the genomes of these two organisms revealed these fungi both encode another copy

of AHAS (AiAHAS and PdAHAS) elsewhere in the genome, which is highly homologous to housekeeping AHAS characterized for fungi. The clustering of a duplicate AHAS^{M}, which has 73% sequence identity to housekeeping AHAS enzymes, indicates the possible role as a self-resistance enzyme (SRE). The clustering of genes encoding SRE with the biosynthetic enzymes of a bioactive natural product is a well-documented occurrence, and has been used to predict function of natural products and for bioactivity-targeted genome mining.[38–41] AHAS catalyzes the first step of branched-chain amino acid biosynthesis, and is the most targeted enzyme for commercial herbicide development.[35, 42–43] We hypothesize that AHAS^{M} enzymes encoded in *A. ibericus* and *P. digitatum* BGCs are the SREs for the products of the clusters, which are expected to be **1** based on the strong homology to *hac* cluster.

Searching through the genomes of Tht22 revealed the presence of two copies of AHAS. Interestingly, one of the AHAS (ThAHAS) is phylogenetically grouped with the canonical housekeeping AHAS found in fungi, while the other (ThAHAS^{M}) groups well with AHAS^{M} found in the *A. ibericus* and *P. digitatum* BGCs (Figure S1A and Table S4). More detailed sequence analysis of AHAS^{M} from the three species showed all three had mutations at P188 (ThAHAS numbering), which is in the active site of AHAS and is a critical resistance-determining residue. When proline is mutated to a small aliphatic amino acid, such as valine or alanine in plant AHAS, the AHAS mutant becomes resistant to most commercial herbicides.[43–46] The corresponding proline residues in ThAHAS^{M}, AiAHAS^{M}, and PdAHAS^{M} are mutated to valine, valine and alanine, respectively (Figure 3A). In contrast, the housekeeping copies of AHAS from these three organisms retain the proline residues.

To compare the activities of the AHAS and AHAS^{M} variants, we recombinantly expressed AHAS of *Arabidopsis thaliana* (NP_190425.1, AtAHAS), *Saccharomyces cerevisiae* (NP_013826.1, SceAHAS), along with ThAHAS and ThAHAS^{M}, using *Escherichia coli* (Figure S4). The kinetic parameters of the AHAS enzymes in converting pyruvate to acetolactate were measured spectroscopically through the conversion of acetolactate to acetoin, as described previously[47–48] and in supporting methods. The kinetic parameters measured for AtAHAS and SceAHAS are comparable to those reported previously (Figure 3C).[45, 49] Both ThAHAS and ThAHAS^{M} display comparable K_M to the other AHAS, however the k_{cat} of ThAHAS^{M} is considerably lower at 0.156 sec^{-1}. When the commercial sulfonylurea sulfometuron methyl (SM) was added to the assays, strong inhibition of AtAHAS and SceAHAS were observed with half-maximal inhibitory concentration (IC_{50}) ~ 30 nM ([E] = 0.5 μM). Similarly, SM potently inhibited ThAHAS with IC_{50} ~ 350 nM. In contrast, no inhibition of ThAHAS^{M} was observed even at elevated concentration (100 μM) of SM, consistent with the presence of the proline to valine mutation. To further investigate the resistance properties of ThAHAS^{M}, we generated a homozygous strain of *S. cerevisiae* that is deleted in *ILV2*, which encodes the yeast AHAS. This strain, unable to grow on Ile and Val dropout media, was transformed with a plasmid expressing either AtAHAS, ThAHAS or ThAHAS^{M}. In all three cases, the complemented yeast strain was able to grow on dropout media (Figure S6C). When SM was added to the yeast cultures, the growth of *Δilv2* strains complemented with AtAHAS and ThAHAS, along with the parent

yeast strain, were potently inhibited (Figure 3B). In contrast, the strain complemented with ThAHAS^{M} showed minimal sensitivity to the presence of SM. Collectively, the *in vivo* and *in vitro* assays confirmed ThAHAS^{M}, with the critical active site proline mutation, is a functional AHAS that is resistant to commercial herbicide. Since AiAHAS^{M} and PdAHAS^{M} are located in the clusters that are homologous to *hac*, we hypothesize that harzianic acid (HA, **1**) is an AHAS inhibitor.

Harzianic acid is a selective inhibitor of fungal AHAS.

The ability of HA to inhibit different AHAS enzymes was tested using purified HA. HA was able to inhibit ThAHAS as a competitive inhibitor with a K_i of 6.65 μM (Figure 3C and S7), which is different from the mixed inhibition modes observed for commercial herbicides.[43] HA only shows weak inhibition towards yeast SceAHAS with a K_i of ~83 μM. No inhibition of plant AtAHAS was observed suggesting HA is a selective fungal AHAS inhibitor. HA was also able to inhibit ThAHAS^{M} with an IC_{50} of 20 μM ([E]=0.5 μM) and a K_i of 3.39 μM. The lack of resistance by ThAHAS^{M} suggests HA binds to AHAS via a completely different mode than the known herbicides, and the proline mutation has no effect on HA:AHAS interactions. Using ThAHAS^{M}, we tested the structural activity relationship (SAR) of HA inhibition. Altering the lengths of the C5' alkyl group has minimal effect, as both **2** and **3** showed comparable IC_{50} as **1**. Removing the *N*-methyl group in **5**, however, led to an increase in IC_{50} to 37 μM (Table S6). We also attempted to assay the in vivo properties of HA using the *S. cerevisiae Δilv2* strain with AHAS complementation, as described for SM in Figure 3B. However, we noted general toxicity of HA towards yeast under assay concentrations, even in Ile and Val supplemented growth media (Figure S6B and S6D). Fungal natural products containing tetramic acids have been noted to cause morphological change in *S. cerevisiae* and induce cell death.[50–51]

Although our initial hypothesis of HA as a AHAS inhibitor is confirmed, inhibition of the proposed SRE ThAHAS^{M} by HA was unexpected. This suggests resistance to HA is not via a completely insensitive SRE. Instead, considering the inhibition of AHAS by HA is weaker compared to other inhibitors, the additional gene encoding AHAS^{M} may increase the level of intracellular AHAS activity to overcome the presence of HA. In addition, a conserved major facilitator superfamily transporter (MFS), HacG (Figure S3), encoded in all three clusters shown in Figure 2A, may facilitate the export of HA to the extracellular space[52].

Structural Basis of ThAHAS Inhibition by Harzianic Acid.

To understand the molecular basis of ThAHAS inhibition by HA, the crystal structures of ThAHAS and ThAHAS-HA complex were determined at resolutions of 2.28 Å and 2.54 Å, respectively (Table S7). Same as SceAHAS (PDB: 1N0H),[53] ThAHAS crystallizes as a homodimer in the asymmetric unit (Figure 4A). The physiological relevance of the dimer structure was confirmed by analytical ultracentrifugation, which showed ThAHAS exists mostly as a dimer in the native state (Figure S10). The overall structures of ThAHAS and ThAHAS-HA complex are almost identical, with a root-mean-square (r.m.s.) deviation of 0.166 Å for 511 Cα atoms between them (Figure S10). The two active sites are located at the dimer interface and are on opposites sides of the complex, as observed in SceAHAS.[54] Unambiguous electron densities for Mg^{2+}, FAD, and thiamine thiazolone diphosphate

(ThThDP) are found in both monomers in both ThAHAS and ThAHAS-HA structures (Figure S12). The isoalloxazine rings of FAD molecules are essentially planar.[55] ThThDP is the C2 oxidized product of thiamine diphosphate (ThDP), which is found in other AHAS structures.[43] Formation of ThThDP can result from direct oxidation by O_2 or through the formation of peracetate-ThDP intermediate, and is a major route to the accumulative inhibition of AHAS in the presence of herbicides.[43, 56]

The electron densities mapped to HA is observed at the entrance of one of the active sites in the ThAHAS-HA complex (Figure S12). HA makes extensive interactions with the dimer interface that forms the substrate entrance tunnel, including numerous hydrophobic interactions and four hydrogen bonds. The substrate entrance channel leads to the active site cavity and ends directly above the C2 atom of ThThDP (Figure 4B). HA complements the shape of the channel by adopting an extended conformation (Figure 4B and 4C). Comparison of uninhibited ThAHAS and ThAHAS-HA complex reveals that while conformations of most residues remain nearly identical, F591 rotates by 5° upon the binding of HA, leading to a slight closure of the entrance tunnel (Figure S11B and S11C). One critical residue positioned at the entrance of channel is K247 from the other monomer (indicated as K247(B)), which not only facilitates hydrophobic interactions with the C2' atoms on the HA tetramic acid ring via its Cε methylene, but also forms a water-mediated hydrogen bond with HA C2' carbonyl group (Figure 4C). The ordered water molecules may be crucial in HA recognition and binding, as no ordered water molecules are seen in the uninhibited ThAHAS structure (Figure S11B). The K247A mutation led to a 4-fold increase in IC_{50} value (162.09 μM) of HA toward ThAHAS (Figure S14A). In addition, Y592 is involved in HA binding by forming hydrogen bonds with the C4' carbonyl group and C7' hydroxyl group. HA forms additional hydrophobic contacts with F197(B), G112(B), and A251(B) to further contribute to the binding.

The binding modes of commercial herbicides to AHAS are similar,[43, 57] but are distinct from that between HA and ThAHAS. Residues lining the middle and deeper portions of the active site entrance tunnel are highly conserved across AHAS of different origins, and define the region that is occupied by commercial herbicides.[46, 53] Shown in Figure 4D is the binding mode of sulfonamide inhibitor metosulam (MT) to *Candida albicans* CalAHAS (PDB: 6DER)[57] (Figure 4D). One overlapping region between MT and HA binding is the cavity defined by conserved W587 and R378 (Figure S13). Recent work has revealed that equivalent residues in *E. coli* AHAS are involved in recognizing 2-ketobutyrate as the second substrate of AHAS-catalyzed reactions.[58] While most residues in the active site adopt nearly identical conformations in ThAHAS-HA and CalAHAS-MT, one significant difference is the side chain orientation of W587. In the CalAHAS-MT complex, the indole ring of W587 rotates 90° to stack with the π system present in the triazolopyrimidine ring of MT (Figure 4D). As a result, MT is buried much deeper in the substrate tunnel with K247(B), W582, and two ordered water molecules collectively form the binding roof; and F197(B) and R376 form the binding floor. Additional anchoring of MT is provided through five hydrogen bonds between the sulfonamide motif and R376, K247(B), and three ordered water molecules. The bend at the sulfonamide group in MT leads to a cation-π interaction between R376 and the phenyl ring in MT. Extensive hydrophobic interactions between MT and CalAHAS[43] are key contributors to the low nanomolar K_i. One, in particular, is

the hydrophobic interaction between the methyl group of MT and A191 Cβ atom (Figure 4D). P188 induces a kink in the polypeptide backbone to enable hydrophobic interactions between A191 and MT methyl group, while also forms a CH-π interaction with MT. P188A substitution abolishes these interactions and hence increases K_i.[56] Considering the structural similarities of commercial AHAS inhibitors and overlapping binding sites as illustrated in Figure 4D, it is therefore not surprising that P188 mutation confers resistance in both plant and fungal AHAS^M.[59–61]

In contrast to commercial herbicides, HA is effective toward ThAHAS^M that contains the resistance-conferring proline to valine mutation because of its drastically different binding mode. This led to the lack of contacts between HA and the pocket lined by P188 and A191 (Figure 4C). Therefore, the binding mode of HA can be rationally exploited in the development of more potent AHAS inhibitors that are effective against widely isolated resistant mutants. Such approaches may include: 1) introduce tetramic acid motif to mediate interactions with additional parts of active site entrance tunnel; 2) derivatize the end of the C3' chain with functional groups such as sulfonamide to establish hydrogen bonds with R378; 3) reconsider the rigid aromatic ring systems found in nearly all commercial herbicides. These π systems, though attractive for potential cation- interactions and π-π stacking to lower K_i, should be strategically incorporated to avoid trapping the inhibitor in the binding cavity defined by the A191 and P188 residues, the latter of which is frequently found to be mutated to confer resistance.

HA inhibits phytopathogenic fungi growth.

AHAS, in addition to being the most targeted enzyme for herbicides, is also an attractive target for antifungal candidate development. AHAS activity is crucial for survival of *Candida albicans* and *Cryptococcus neoformans* in vitro, and BCAA auxotrophic strains of these two fungal pathogens are avirulent in vivo.[61–62] Commercial AHAS-targeting herbicides, given their broad spectrum activity, are also potent inhibitors of fungal AHAS[57, 63–64]. In contrast, HA displays selective inhibition towards fungal housekeeping AHAS and resistant AHAS^M (Figure 3C), and has no activity towards plant AHAS. This trait makes HA a particularly viable candidate for targeting phytopathogenic fungi in the rhizosphere, and suggests this could be one of the biological functions of the molecule. Indeed, previous work with pure HA demonstrates antifungal activities towards a panel of phytopathogens.[26]

We compared the sequences of housekeeping AHAS from different plant pathogenic fungi, such as those from *F. oxysporium and S. sclerotiorum* (Figures 3A and S9). Interestingly, the only copy of AHAS in these species all contain the resistant-determining P188 (ThAHAS numbering) mutation to valine, thus indicating these strains should be resistant to commercial AHAS inhibitors. To assay the AHAS activities, we recombinantly expressed and purified AHAS from *F. oxysporum* NRRL 32931 (FuoAHAS) and *S. sclerotiorum* 1980 UF-70 (ScsAHAS). The K_M and k_{cat} values were comparable to those of AtAHAS and ThAHAS (Figure 3C). As expected from the proline to valine mutation, both FuoAHAS and ScsAHAS were completely insensitive to SM under in vitro assay conditions. In contrast, HA displayed K_i values of 13.96 μM and 10.99 μM towards FuoAHAS and ScsAHAS,

respectively (Figure 3C and Figure S8), which are similar to the K_i measured towards ThAHAS. Next we evaluated the antifungal activity of HA towards *F. oxysporum* by using the resazurin assay.[65] When the fungus was grown in the presence of BCCAs (Leu, Ile and Val), inhibition of growth was only observed at very high concentrations of HA (Figure 5A). However, upon removing the BCCAs from the growth medium, HA effectively inhibited the growth of *F. oxysporum* with an IC_{50} of ~26 μg/mL. Therefore, although the antifungal potency of HA is not high under the assay conditions, it is evident that HA could target the BCAA pathway and inhibit the growth of phytopathogenic fungi that are otherwise resistant to commercial AHAS herbicides.

The molecular basis for the selectivity of HA towards fungal AHAS can be rationalized by sequence and structure comparisons. We modeled HA into AtAHAS and SceAHAS based on the crystal structure of the ThAHAS-HA complex (Figure 4E). Unlike the broad-spectrum inhibitor MT that is buried deeper, HA interacts with residues at the entrance of channel that are exposed to the solvent, including A251 and Y592 (Figure 4C). Plant and fungal AHASs diverge significantly in identities of residues in this region, in contrast to the high sequence identity closer to the active site area (Figure S15). A251 that is conserved in filamentous fungi (and yeast) corresponds to Q260 in the plant AtAHAS, while a non-interacting residue P116 corresponds to E125 in AtAHAS (Figure 4E). The bulkier side chains of these residues in AtAHAS narrow the substrate entrance tunnel considerably. This constriction leads to steric clashes with C6' methylene group and C7' hydroxyl group of HA (Figure 4E), and hence prevents the binding of HA to AtAHAS. One potential contributor to the HA preferential binding (> 10 fold lower in K_i) to filamentous fungal AHAS over yeast SceAHAS is the *C*-terminal loop A658-H663 in ThAHAS (Figure 4E). The 3.6-Å distance between A658 Cβ atom and HA C2' carbonyl oxygen atom indicates van der Waals interaction. In contrast, the corresponding amino acid G653 in SceAHAS is located 5.3-Å away. It is worth noting that G657A substitution increases the sensitivity of SceAHAS to imidazolinone herbicides.[45] Our modeling study echoes this previous report that enabling interactions at this position with an alanine substitution can improve inhibition.

Although a complete picture of HA role in the rhizosphere is still lacking due to its multitude of physical and biological properties, our studies suggest one role of this natural product from Tht22 may be to limit the growth of competing fungi, especially phytopathogenic ones, through the selective inhibition of AHAS (Figure 5B). This antagonist role towards harmful fungi may be synergistically combined with the strong iron-binding properties of HA to improve plant fitness. The lack of HA binding to plant AHAS also ensures that HA does not harm plant growth. It is important to note that the pathogenic fungal species examined here all contain the proline to valine mutation, which make them resistant to commercial herbicides and other AHAS inhibitors that have similar modes of binding. The timing of emergence of such mutations in these soil fungi is unclear, although certainly precedes the wide spread application of AHAS herbicide in the field. Therefore, it is possible that filamentous fungi have evolved the AHAS to be resistant to some natural product inhibitor (yet to be found) that targets deep in the active site tunnel, and the proline substitution is the most effective resistance-conferring mutation. Tht22 and other producers of HA, however, in a small-molecule arms races, may have evolved and acquired the HA biosynthetic pathway to overcome such resistance.

Summary

In this report, we reconstituted the biosynthesis of harzianic acid (HA), a natural product known to modulate plant-fungus and fungus-fungus interactions from *Trichoderma afroharzianum* t-22, using *A. nidulans* as a heterologous host. Using the BGC information and homologous clusters from other fungi, we hypothesized HA may be an inhibitor of the AHAS, the enzyme catalyzing the first step of branched-chain amino acid biosynthesis. Biochemical assays validated the hypothesis and showed HA is a selective inhibitor of AHAS from filamentous fungi, including the $AHAS^{M}$ variants that are resistant to commercial herbicides with the key proline to valine mutation. HA does not display any inhibition towards plant AHAS. The structural basis of HA inhibition was visualized by the HA-AHAS cocrystal structure, in which HA binds in a distinct orientation than the commercial herbicides. The cocrystal structure also provided explanation to the selectivity of HA, as well as the inhibitory activities towards resistant AHAS mutants. We propose one role of HA in the rhizosphere could be to target the housekeeping AHASs in phytopathogenic fungi that have evolved to be resistant to other AHAS inhibitors. Overall, our genome mining, biochemical assay and structural biology work demonstrate HA as a new natural product inhibitor of AHAS, one of the most sought-after target in the development of herbicides.

Supplementary Material

Refer to Web version on PubMed Central for supplementary material.

ACKNOWLEDGMENT

We thank Dr. J. Clardy for providing *T. afroharzianum* t-22 strain. This work was supported by grant #1025336 from the National Institute of Food and Agriculture and R35GM118056 from NIH to Y.T. L.X. is a visiting student supported by a fellowship from the China Scholarship Council (no. 201903250087).

REFERENCES

(1). Scherlach K; Hertweck C Triggering cryptic natural product biosynthesis in microorganisms. Org. Biomol. Chem 2009, 7 (9), 1753–1760. [PubMed: 19590766]

(2). Schueffler A; Anke T Fungal natural products in research and development. Nat. Prod. Rep 2014, 31 (10), 1425–1448. [PubMed: 25122538]

(3). Dayan FE; Cantrell CL; Duke SO Natural products in crop protection. Bioorg. Med. Chem 2009, 17 (12), 4022–4034. [PubMed: 19216080]

(4). Nisa H; Kamili AN; Nawchoo IA; Shafi S; Shameem N; Bandh SA Fungal endophytes as prolific source of phytochemicals and other bioactive natural products: a review. Microb. Pathog 2015, 82, 50–59. [PubMed: 25865953]

(5). Vinale F; Manganiello G; Nigro M; Mazzei P; Piccolo A; Pascale A; Ruocco M; Marra R; Lombardi N; Lanzuise S A novel fungal metabolite with beneficial properties for agricultural applications. Molecules 2014, 19 (7), 9760–9772. [PubMed: 25006784]

(6). Sparks TC; Hahn DR; Garizi NV Natural products, their derivatives, mimics and synthetic equivalents: role in agrochemical discovery. Pest Manag. Sci 2017, 73 (4), 700–715. [PubMed: 27739147]

(7). Mauch-Mani B; Mauch F The role of abscisic acid in plant–pathogen interactions. Curr. Opin. Plant Biol 2005, 8 (4), 409–414. [PubMed: 15939661]

(8). Gutiérrez-Mañero FJ; Ramos-Solano B; Probanza A. n.; Mehouachi J; R. Tadeo F; Talon M The plant-growth-promoting rhizobacteria *Bacillus pumilus* and *Bacillus licheniformis* produce high amounts of physiologically active gibberellins. Physiol. Plant 2001, 111 (2), 206–211.

(9). Pharis RP; King RW Gibberellins and reproductive development in seed plants. Annu. Rev. Plant Physiol 1985, 36 (1), 517–568.

(10). Vinale F; Sivasithamparam K; Ghisalberti EL; Woo SL; Nigro M; Marra R; Lombardi N; Pascale A; Ruocco M; Lanzuise S *Trichoderma* secondary metabolites active on plants and fungal pathogens. Open Mycol J 2014, 8 (1), 127–139.

(11). Vinale F; Ghisalberti E; Sivasithamparam K; Marra R; Ritieni A; Ferracane R; Woo S; Lorito M Factors affecting the production of *Trichoderma* harzianum secondary metabolites during the interaction with different plant pathogens. Lett. Appl. Microbiol 2009, 48 (6), 705–711. [PubMed: 19413806]

(12). Chaverri P; Branco-Rocha F; Jaklitsch W; Gazis R; Degenkolb T; Samuels GJ Systematics of the *Trichoderma harzianum* species complex and the re-identification of commercial biocontrol strains. Mycologia 2015, 107 (3), 558–590. [PubMed: 25661720]

(13). Harman GE Myths and dogmas of biocontrol changes in perceptions derived from research on *Trichoderma harzinum* T-22. Plant Dis. 2000, 84 (4), 377–393. [PubMed: 30841158]

(14). Vitti A; Pellegrini E; Nali C; Lovelli S; Sofo A; Valerio M; Scopa A; Nuzzaci M *Trichoderma harzianum* T-22 induces systemic resistance in tomato infected by Cucumber mosaic virus. Front. Plant Sci 2016, 7, 1520. [PubMed: 27777581]

(15). Shoresh M; Harman GE. The molecular basis of shoot responses of maize seedlings to *Trichoderma harzianum* T22 inoculation of the root: a proteomic approach. Plant Physiol. 2008, 147 (4), 2147–2163. [PubMed: 18562766]

(16). Mastouri F; Björkman T; Harman GE Seed treatment with *Trichoderma harzianum* alleviates biotic, abiotic, and physiological stresses in germinating seeds and seedlings. Phytopathology 2010, 100 (11), 1213–1221. [PubMed: 20649416]

(17). Innocenti G; Roberti R; Piattoni F Biocontrol ability of *Trichoderma harzianum* strain T22 against Fusarium wilt disease on water-stressed lettuce plants. BioControl 2015, 60 (4), 573–581.

(18). Harman GE; Petzoldt R; Comis A; Chen J Interactions between *Trichoderma harzianum* strain T22 and maize inbred line Mo17 and effects of these interactions on diseases caused by Pythium ultimum and Colletotrichum graminicola. Phytopathology 2004, 94 (2), 147–153. [PubMed: 18943537]

(19). Sofo A; Scopa A; Manfra M; De Nisco M; Tenore G; Troisi J; Di Fiori R; Novellino E *Trichoderma harzianum* strain T-22 induces changes in phytohormone levels in cherry rootstocks (Prunus cerasus× P. canescens). Plant Growth Regul. 2011, 65 (2), 421–425.

(20). Marfori EC; Kajiyama S i.; Fukusaki, E.-i.; Kobayashi, A. Trichosetin, a novel tetramic acid antibiotic produced in dual culture of *Trichoderma harzianum* and *Catharanthus roseus* callus. Z. Naturforsch. C 2002, 57 (5–6), 465–470. [PubMed: 12132686]

(21). Cai F; Yu G; Wang P; Wei Z; Fu L; Shen Q; Chen W Harzianolide, a novel plant growth regulator and systemic resistance elicitor from *Trichoderma harzianum*. Plant Physiol. Biochem 2013, 73, 106–113. [PubMed: 24080397]

(22). Keswani C; Mishra S; Sarma BK; Singh SP; Singh HB Unraveling the efficient applications of secondary metabolites of various *Trichoderma* spp. Appl. Microbiol. Biotechnol 2014, 98 (2), 533–544. [PubMed: 24276619]

(23). Vinale F; Marra R; Scala F; Ghisalberti E; Lorito M; Sivasithamparam K Major secondary metabolites produced by two commercial *Trichoderma* strains active against different phytopathogens. Lett. Appl. Microbiol 2006, 43 (2), 143–148. [PubMed: 16869896]

(24). Nordberg H; Cantor M; Dusheyko S; Hua S; Poliakov A; Shabalov I; Smirnova T; Grigoriev IV; Dubchak I The genome portal of the Department of Energy Joint Genome Institute: 2014 updates. Nucleic Acids Res. 2014, 42 (D1), D26–D31. [PubMed: 24225321]

(25). Chen M; Liu Q; Gao S-S; Young AE; Jacobsen SE; Tang Y Genome mining and biosynthesis of a polyketide from a biofertilizer fungus that can facilitate reductive iron assimilation in plant. Proc. Natl. Acad. Sci. U.S.A 2019, 116 (12), 5499–5504. [PubMed: 30842286]

(26). Vinale F; Flematti G; Sivasithamparam K; Lorito M; Marra R; Skelton BW; Ghisalberti EL Harzianic acid, an antifungal and plant growth promoting metabolite from *Trichoderma harzianum*. J. Nat. Prod 2009, 72 (11), 2032–2035. [PubMed: 19894739]

(27). Sawa R; Mori Y; Iinuma H; Naganawa H; Hamada M; Yoshida S; Furutani H; Kajimura Y; Fuwa T; Takeuchi T Harzianic acid, a new antimicrobial antibiotic from a fungus. J. Antibiot 1994, 47 (6), 731–732.

(28). Kawada M; Yoshimoto Y; Kumagai H; Someno T; Momose I; Kawamura N; Isshiki K; Ikeda D PP2A inhibitors, harzianic acid and related compounds produced by fungus strain F-1531. J. Antibiot 2004, 57 (3), 235–237.

(29). Vinale F; Nigro M; Sivasithamparam K; Flematti G; Ghisalberti EL; Ruocco M; Varlese R; Marra R; Lanzuise S; Eid A Harzianic acid: a novel siderophore from *Trichoderma harzianum*. FEMS Microbiol. Lett 2013, 347 (2), 123–129. [PubMed: 23909277]

(30). Marra R; Lombardi N; d'Errico G; Troisi J; Scala G; Vinale F; Woo SL; Bonanomi G; Lorito M Application of *Trichoderma* strains and metabolites enhances soybean productivity and nutrient content. J. Agric. Food. Chem 2019, 67 (7), 1814–1822. [PubMed: 30657682]

(31). Sims JW; Fillmore JP; Warner DD; Schmidt EW Equisetin biosynthesis in *Fusarium heterosporum*. ChemComm 2005, (2), 186–188.

(32). Kakule TB; Zhang S; Zhan J; Schmidt EW Biosynthesis of the tetramic acids Sch210971 and Sch210972. Org. Lett 2015, 17 (10), 2295–2297. [PubMed: 25885659]

(33). Zhu Y; Wang J; Mou P; Yan Y; Chen M; Tang Y Genome mining of cryptic tetronate natural products from a PKS-NRPS encoding gene cluster in *Trichoderma harzianum* t-22. Org. Biomol. Chem. Chemistry 2021, 19, 1985–1990.

(34). Pang SS; Duggleby RG; Guddat LW Crystal structure of yeast acetohydroxyacid synthase: a target for herbicidal inhibitors. J. Mol. Biol 2002, 317 (2), 249–262. [PubMed: 11902841]

(35). Duggleby RG; Pang SS Acetohydroxyacid synthase. J. Biochem. Mol. Biol 2000, 33 (1), 1–36.

(36). Liu N; Hung Y-S; Gao S-S; Hang L; Zou Y; Chooi Y-H; Tang Y Identification and heterologous production of a benzoyl-primed tricarboxylic acid polyketide intermediate from the zaragozic acid A biosynthetic pathway. Org. Lett 2017, 19 (13), 3560–3563. [PubMed: 28605916]

(37). Healy AR; Vinale F; Lorito M; Westwood NJ Total synthesis and biological evaluation of the tetramic acid based natural product harzianic acid and its stereoisomers. Org. Lett 2015, 17 (3), 692–695. [PubMed: 25629709]

(38). Yan Y; Liu Q; Zang X; Yuan S; Bat-Erdene U; Nguyen C; Gan J; Zhou J; Jacobsen SE; Tang Y Resistance-gene-directed discovery of a natural-product herbicide with a new mode of action. Nature 2018, 559 (7714), 415–418. [PubMed: 29995859]

(39). Yan Y; Liu N; Tang Y Recent developments in self-resistance gene directed natural product discovery. Nat. Prod. Rep 2020, 37, 879–892. [PubMed: 31912842]

(40). Panter F; Krug D; Baumann S; Müller R Self-resistance guided genome mining uncovers new topoisomerase inhibitors from myxobacteria. Chem. Sci 2018, 9 (21), 4898–4908. [PubMed: 29910943]

(41). Yeh H-H; Ahuja M; Chiang Y-M; Oakley CE; Moore S; Yoon O; Hajovsky H; Bok J-W; Keller NP; Wang CC Resistance gene-guided genome mining: serial promoter exchanges in Aspergillus nidulans reveal the biosynthetic pathway for fellutamide B, a proteasome inhibitor. ACS Chem. Biol 2016, 11 (8), 2275–2284. [PubMed: 27294372]

(42). McCourt J; Duggleby R Acetohydroxyacid synthase and its role in the biosynthetic pathway for branched-chain amino acids. Amino acids 2006, 31 (2), 173–210. [PubMed: 16699828]

(43). Garcia MD; Nouwens A; Lonhienne TG; Guddat LW Comprehensive understanding of acetohydroxyacid synthase inhibition by different herbicide families. Proc. Natl. Acad. Sci. U.S.A 2017, 114 (7), E1091–E1100. [PubMed: 28137884]

(44). Duggleby RG; McCourt JA; Guddat LW Structure and mechanism of inhibition of plant acetohydroxyacid synthase. Plant Physiol. Biochem 2008, 46 (3), 309–324. [PubMed: 18234503]

(45). Duggleby RG; Pang SS; Yu H; Guddat LW Systematic characterization of mutations in yeast acetohydroxyacid synthase: interpretation of herbicide-resistance data. Eur. j. biochem 2003, 270 (13), 2895–2904. [PubMed: 12823560]

(46). McCourt JA; Pang SS; King-Scott J; Guddat LW; Duggleby RG Herbicide-binding sites revealed in the structure of plant acetohydroxyacid synthase. Proc. Natl. Acad. Sci. U.S.A 2006, 103 (3), 569–573. [PubMed: 16407096]

(47). Simpson DM; Stoller EW; Wax LM An in vivo acetolactate synthase assay. Weed Technol 1995, 17–22.

(48). Westerfeld W A colorimetric determination of blood acetoin. J. Biol. Chem 1945, 161 (2), 495–502. [PubMed: 21006932]

(49). Pang SS; Duggleby RG Expression, purification, characterization, and reconstitution of the large and small subunits of yeast acetohydroxyacid synthase. Biochemistry 1999, 38 (16), 5222–5231. [PubMed: 10213630]

(50). Sakai K; Unten Y; Iwatsuki M; Matsuo H; Fukasawa W; Hirose T; Chinen T; Nonaka K; Nakashima T; Sunazuka T Fusaramin, an antimitochondrial compound produced by *Fusarium* sp., discovered using multidrug-sensitive *Saccharomyces cerevisiae*. J. Antibiot 2019, 72 (9), 645–652.

(51). Lowery CA; Park J; Gloeckner C; Meijler MM; Mueller RS; Boshoff HI; Ulrich RL; Barry III CE; Bartlett DH; Kravchenko VV Defining the mode of action of tetramic acid antibacterials derived from Pseudomonas aeruginosa quorum sensing signals. J. Am. Chem. Soc 2009, 131 (40), 14473–14479. [PubMed: 19807189]

(52). Almabruk KH; Dinh LK; Philmus B Self-resistance of natural product producers: past, present, and future focusing on self-resistant protein variants. ACS Chem. Biol 2018, 13 (6), 1426–1437. [PubMed: 29763292]

(53). Pang SS; Guddat LW; Duggleby RG Molecular basis of sulfonylurea herbicide inhibition of acetohydroxyacid synthase. J. Biol. Chem 2003, 278 (9), 7639–7644. [PubMed: 12496246]

(54). Lonhienne T; Garcia MD; Noble C; Harmer J; Fraser JA; Williams CM; Guddat LW High Resolution Crystal Structures of the Acetohydroxyacid Synthase-Pyruvate Complex Provide New Insights into Its Catalytic Mechanism. ChemistrySelect 2017, 2 (36), 11981–11988.

(55). Lonhienne T; Garcia MD; Fraser JA; Williams CM; Guddat LW The 2.0 Å X-ray structure for yeast acetohydroxyacid synthase provides new insights into its cofactor and quaternary structure requirements. PLoS One 2017, 12 (2), e0171443. [PubMed: 28178302]

(56). Lonhienne T; Garcia MD; Pierens G; Mobli M; Nouwens A; Guddat LW Structural insights into the mechanism of inhibition of AHAS by herbicides. Proc. Natl. Acad. Sci. U.S.A 2018, 115 (9), E1945–E1954. [PubMed: 29440497]

(57). Garcia MD; Chua SM; Low Y-S; Lee Y-T; Agnew-Francis K; Wang J-G; Nouwens A; Lonhienne T; Williams CM; Fraser JA Commercial AHAS-inhibiting herbicides are promising drug leads for the treatment of human fungal pathogenic infections. Proc. Natl. Acad. Sci. U.S.A 2018, 115 (41), E9649–E9658. [PubMed: 30249642]

(58). Tittmann K; Vyazmensky M; Hübner G; Barak Z. e.; Chipman DM The carboligation reaction of acetohydroxyacid synthase II: steady-state intermediate distributions in wild type and mutants by NMR. Proc. Natl. Acad. Sci. U.S.A 2005, 102 (3), 553–558. [PubMed: 15640355]

(59). Tranel PJ; Wright TR Resistance of weeds to ALS-inhibiting herbicides: what have we learned? Weed Sci. 2002, 50 (6), 700–712.

(60). Richie DL; Thompson KV; Studer C; Prindle VC; Aust T; Riedl R; Estoppey D; Tao J; Sexton JA; Zabawa T Identification and evaluation of novel acetolactate synthase inhibitors as antifungal agents. Antimicrob. Agents Chemother 2013, 57 (5), 2272–2280. [PubMed: 23478965]

(61). Kingsbury JM; Yang Z; Ganous TM; Cox GM; McCusker JH *Cryptococcus neoformans* Ilv2p confers resistance to sulfometuron methyl and is required for survival at 37 °C and in vivo. Microbiology 2004, 150 (5), 1547–1558. [PubMed: 15133116]

(62). Kingsbury JM; McCusker JH Cytocidal amino acid starvation of *Saccharomyces cerevisiae* and *Candida albicans* acetolactate synthase (*ilv2Δ*) mutants is influenced by the carbon source and rapamycin. Microbiology 2010, 156 (Pt 3), 929. [PubMed: 20019084]

(63). Lee Y-T; Cui C-J; Chow EW; Pue N; Lonhienne T; Wang J-G; Fraser JA; Guddat LW Sulfonylureas have antifungal activity and are potent inhibitors of *Candida albicans* acetohydroxyacid synthase. J. Med. Chem 2013, 56 (1), 210–219. [PubMed: 23237384]

(64). Agnew-Francis KA; Tang Y; Lin X; Low YS; Wun SJ; Kuo A; Elias SSI; Lonhienne T; Condon ND; Pimentel BN Herbicides That Target Acetohydroxyacid Synthase Are Potent Inhibitors of the Growth of Drug-Resistant *Candida auris*. ACS Infect. Dis 2020, 6 (11), 2901–2912. [PubMed: 32986949]

(65). Monteiro MC; de la Cruz M; Cantizani J; Moreno C; Tormo JR; Mellado E; De Lucas JR; Asensio F; Valiante V; Brakhage AA A new approach to drug discovery: high-throughput screening of microbial natural extracts against *Aspergillus fumigatus* using resazurin. J Biomol Screen 2012, 17 (4), 542–549. [PubMed: 22233645]

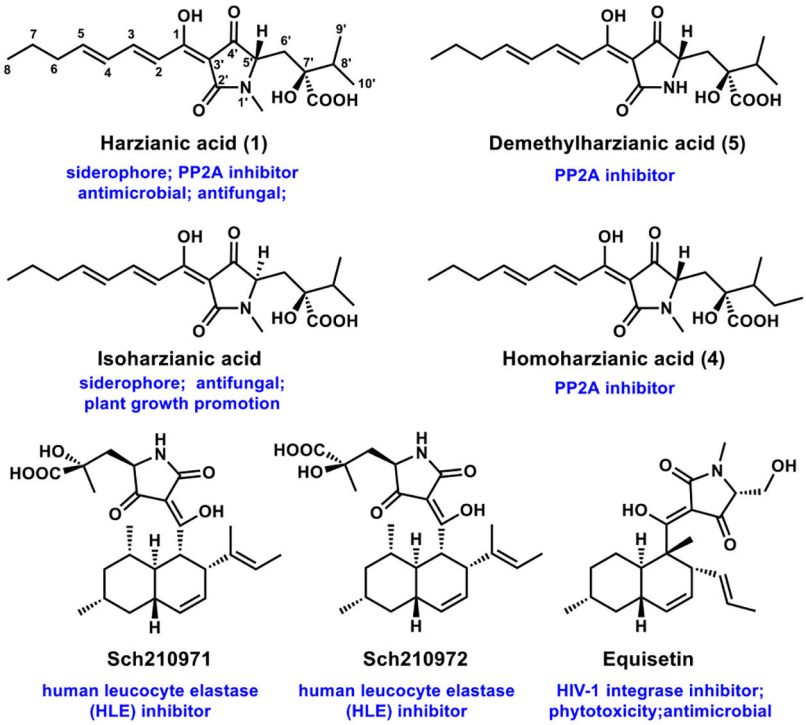

Figure 1.

Harzianic acid (**1**) and derivatives are tetramic acids isolated from fungi. Other compounds with structural features related to harzianic acid are shown in the third row. All these compounds are biosynthesized from polyketide synthase-nonribosomal peptide synthetase (PKS-NRPS) pathways.

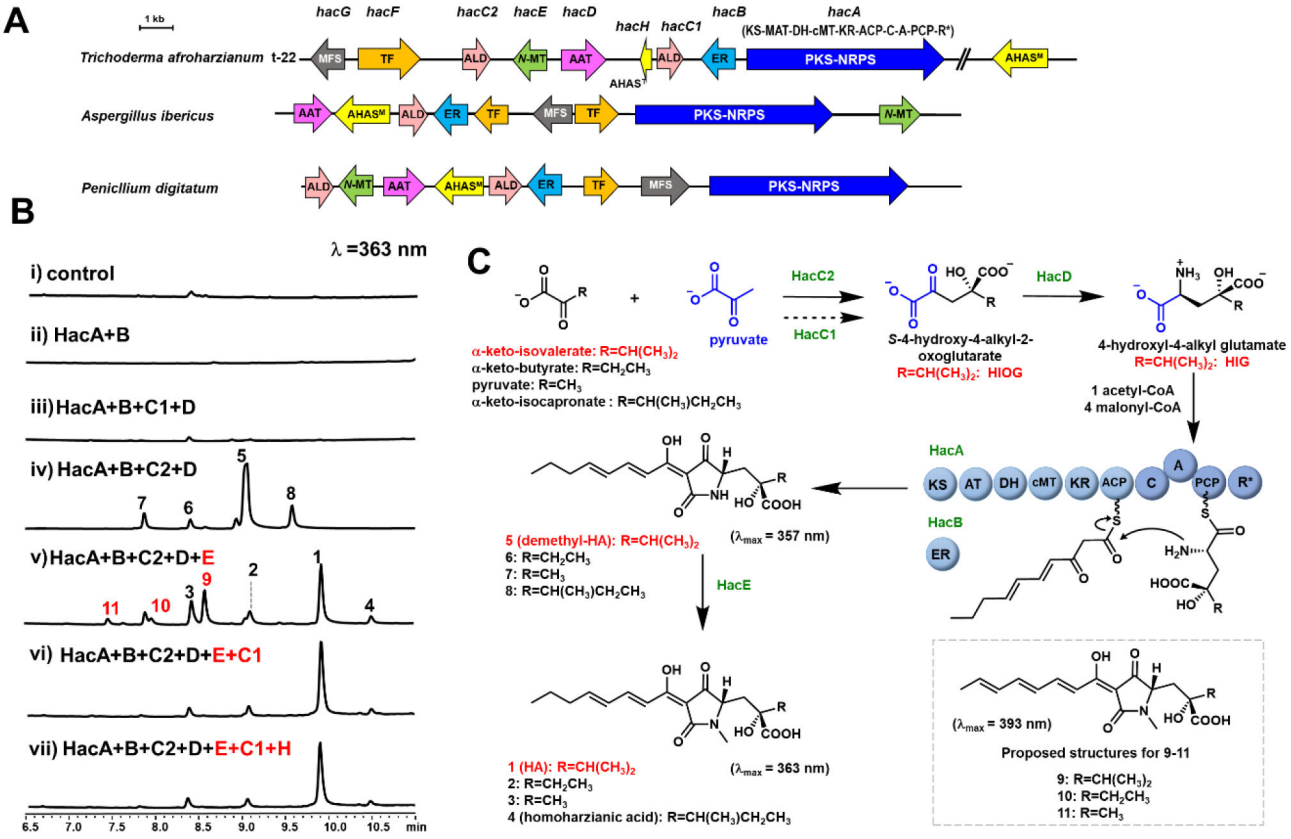

Figure 2.

Proposed biosynthetic pathway of HA. (**A**) Comparison of the ThT22 HA BGC with homologous BGCs from *A. ibericus* and *P. digitatum*. Abbreviations: KS, ketosynthase; MAT, malonyl-CoA:ACP transacylase; DH, dehydratase; cMT, C-methyltransferase; KR, ketoreductase; ACP, acyl-carrier protein; C, condensation; A, adenylation; PCP, peptidyl-carrier protein; R*, Dieckmann cyclization; TF, transcriptional factor; MFS, major facilitator superfamily transporter; ALD, aldolase; *N*-MT, *N*-methyltransferase; AAT; aminotransferase (transaminase); ER; *trans*-enoylreductase; AHAS, acetohydroxyacid synthase.(**B**) LC-MS traces of metabolites produced by the heterologous host *A. nidulans*. For each trace, the gene indicated in red represents addition from the previous combination. (**C**) Putative biosynthetic pathway of HA and congeners.

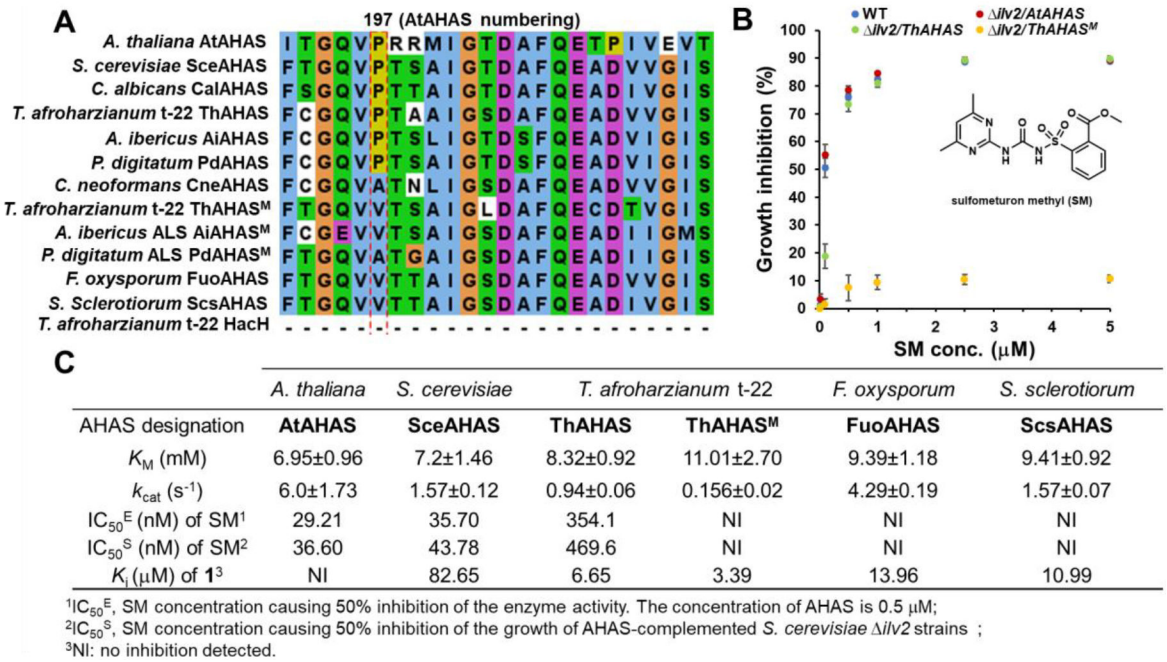

C

	A. thaliana	*S. cerevisiae*	*T. afroharzianum* t-22		*F. oxysporum*	*S. sclerotiorum*
AHAS designation	**AtAHAS**	**SceAHAS**	**ThAHAS**	**ThAHAS^M**	**FuoAHAS**	**ScsAHAS**
K_M (mM)	6.95±0.96	7.2±1.46	8.32±0.92	11.01±2.70	9.39±1.18	9.41±0.92
k_{cat} (s^{-1})	6.0±1.73	1.57±0.12	0.94±0.06	0.156±0.02	4.29±0.19	1.57±0.07
IC_{50}^E (nM) of SM[1]	29.21	35.70	354.1	NI	NI	NI
IC_{50}^S (nM) of SM[2]	36.60	43.78	469.6	NI	NI	NI
K_i (μM) of **1**[3]	NI	82.65	6.65	3.39	13.96	10.99

[1]IC_{50}^E, SM concentration causing 50% inhibition of the enzyme activity. The concentration of AHAS is 0.5 μM;
[2]IC_{50}^S, SM concentration causing 50% inhibition of the growth of AHAS-complemented *S. cerevisiae* Δ*ilv2* strains ;
[3]NI: no inhibition detected.

Figure 3.

AHAS^M is resistant to commercial herbicides. (**A**) Multiple sequence alignment of AHASs from different organisms. (**B**) Growth-inhibition curves of sulfometuron methyl (SM) on *S. cerevisiae* BJ5464-NpgA (blue) and *Δilv2* strains expressing AtAHAS (red), ThAHAS (green) and ThAHAS^M (yellow) when cultured in isoleucine and valine (I, V) dropout SDct medium. Data are mean ± s.d. from three biologically independent experiments. (**C**) Kinetic and inhibition characterization of SM and **1** toward AHAS.

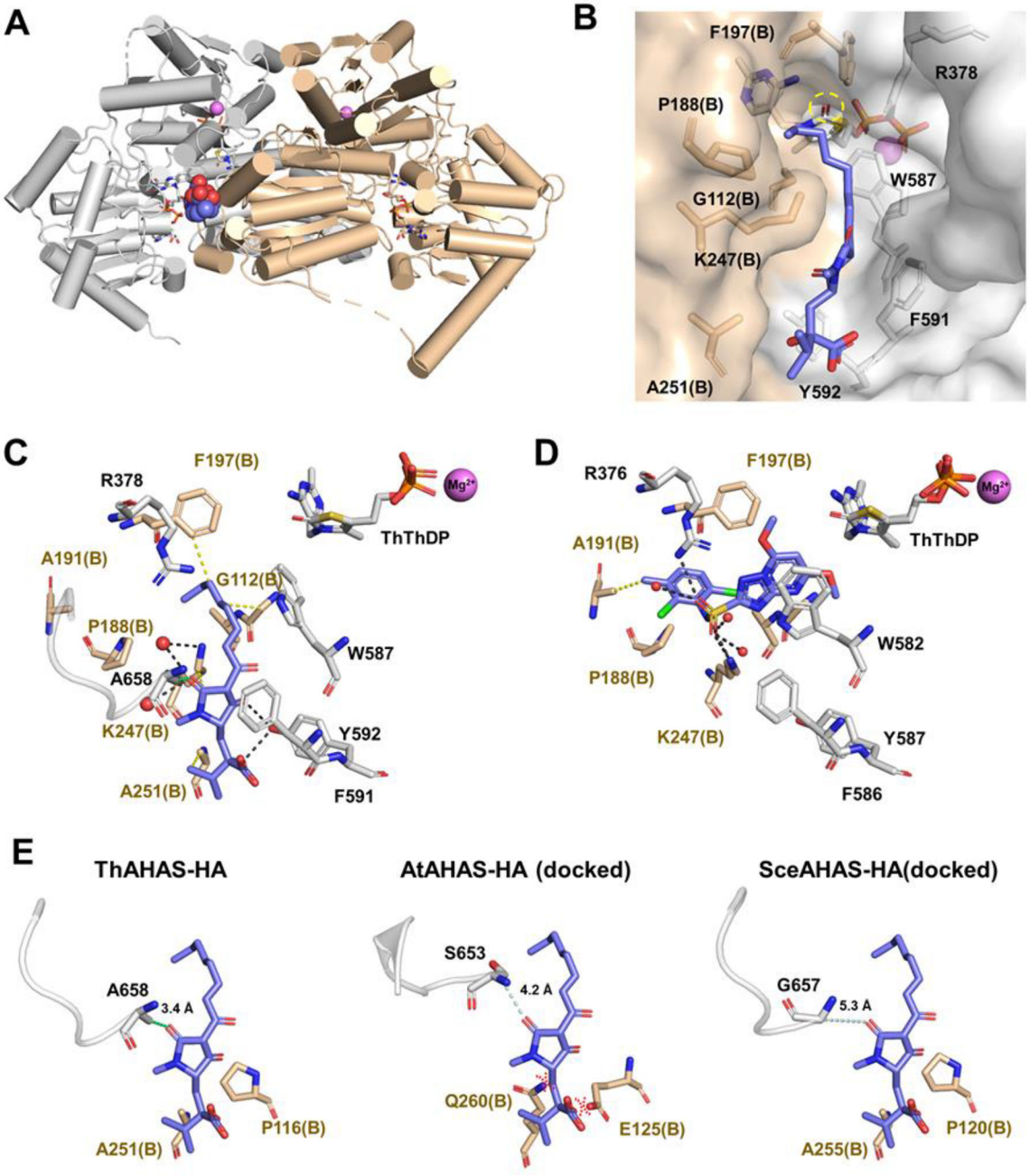

Figure 4.

Crystal structure of ThAHAS-HA complex. (**A**) ThAHAS is crystallized as a dimer. Mg^{2+} ions are shown as pink spheres, FAD and ThThDP are color-coded the same way as the corresponding monomer, and HA is shown in blue and red spheres. (**B**) HA is in an extended conformation at the active site entrance tunnel defined by the dimer interface. The C2 carbonyl of thiamine thiazolone diphosphate (ThThDP) is circled in dashed yellow lines. (**C**) A detailed view of interactions between HA and ThAHAS in the complex. Black dashed lines represent hydrogen bonds, yellow dashed lines represent hydrophobic interactions, green dashed lines represent van der Waals interactions, and water molecules

are shown as red spheres. Residues from each monomer are color-coded the same way as the corresponding monomers in (A). (**D**) The binding mode of commercial herbicide MT to CalAHAS (PDB: 6DER) is distinct from that of HA. The overall structures of ThAHAS and CalAHAS share a high similarity, with a r.m.s. deviation is 0.395 Å for 487 Cα atoms. Only one hydrophobic interaction between A191 and MT is shown, which is in yellow dashed lines. The remaining ~25 hydrophobic interactions are omitted for clarity. Hydrogen bonds are shown in black dashed lines. (**E**) Modeling HA into AtAHAS (PDB: 3E9Y) and SceAHAS (PDB: 1N0H) revealed molecular basis of HA selectivity for fungal AHAS. The r.m.s. deviation is 0.410 Å for 486 Cα atoms between ThAHAS and SceAHAS. A658 forms van der Waals interaction (shown in green dashed lines) with HA C2' carbonyl oxygen. Such interaction is absent in SceAHAS or AtAHAS, as the distances are indicated in cyan dashed lines. The sidechains of E125 and Q260 in AtAHAS (equivalent to P116 and A251 in ThAHAS) significantly narrow the active site entrance tunnel where HA binds and lead to steric clashes with HA (shown in red dashed lines).

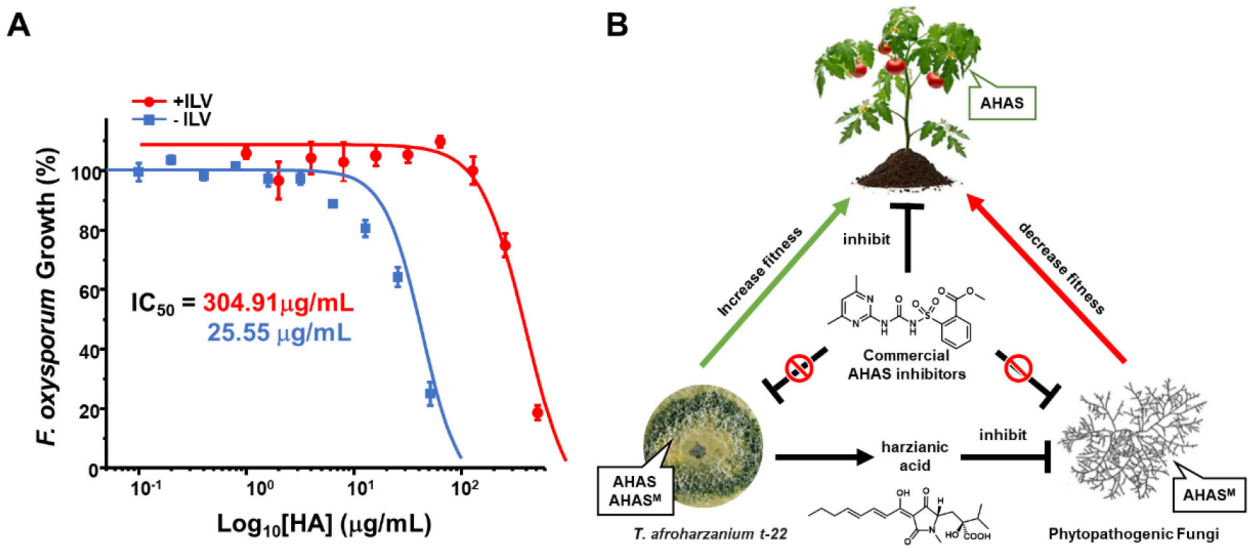

Figure 5.

HA inhibits pathogenic fungi growth. (**A**) Percentage of *f. oxysporum* growth with HA after 48h in RPMI 1640 medium with or without BCAAs. (**B**) A possible role of HA to limit phytopathogenic fungi growth in the rhizosphere.